Modeling Tradable Credit Scheme for Multimodal Urban Networks with Departure Time: a Bathtub Approach

Louis Balzer, Mostafa Ameli, Ludovic Leclercq, Jean-Patrick Lebacque

MODELING TRADABLE CREDIT SCHEME FOR MULTIMODAL URBAN NETWORKS WITH DEPARTURE TIME: A BATHTUB APPROACH

Louis Balzer, Corresponding Author
Univ. Gustave Eiffel, ENTPE, LICIT-ECO7, Lyon, France
https://orcid.org/0000-0002-9638-7478
louis.balzer@univ-eiffel.fr

Mostafa Ameli
Univ. Gustave Eiffel, COSYS, GRETTIA, Paris, France
https://orcid.org/0000-0002-2470-6812
mostafa.ameli@univ-eiffel.fr

Ludovic Leclercq
Univ. Gustave Eiffel, ENTPE, LICIT-ECO7, Lyon, France
https://orcid.org/0000-0002-3942-6354
ludovic.leclercq@univ-eiffel.fr

Jean-Patrick Lebacque
Univ. Gustave Eiffel, COSYS, GRETTIA, Paris, France
https://orcid.org/0000-0002-5339-5988
jean-patrick.lebacque@univ-eiffel.fr

Paper submitted for presentation at the 102nd Annual Meeting Transportation Research Board, Washington D.C., January 2023.

Paper submitted to the Transportation Research Board ACP50 Standing Committee on "Traffic Flow Theory and Characteristics".

CONFLICT OF INTEREST

The authors declare no potential conflict of interests.

AUTHOR CONTRIBUTION STATEMENT

The authors confirm contribution to the paper as follows: study conception and design: LB, MA, LL, JPL; data collection: LB, MA, LL; analysis and interpretation of results: LB, MA; draft manuscript preparation: LB, MA; All authors reviewed the results and approved the final version of the manuscript.

Word Count: 6997 words + 2 table(s) $\times$ 250 = 7497 words

Submission Date: August 1, 2022

ABSTRACT

A Tradable Credit Scheme (TCS) is a demand management policy aiming for more sustainable travel behaviors. The regulator defines the total credit cap and the credit distribution among the population. It also determines the required credit charges for each travel alternative at different times of the day, which modifies the perceived travel costs by users. The credit price is determined by the trade of credits between travelers. Defining the credit scheme at the urban level and estimating its impacts on user travel decisions and the network congestion dynamics is challenging. We propose a modeling framework wherein travelers change their departure times and choose between solo car driving, Public Transportation (PT), and carpooling to complete their trips under a dynamic TCS, meaning the credit charge is time-dependent. This framework extends the generalized bathtub model to capture the congestion dynamics for the different transport modes. Additionally, we consider different values of time, trip lengths, and desired arrival times for the demand profile.

The modeling framework enables us to find the optimal credit charge to minimize the congestion cost (the sum of all travelers' schedule costs) and the carbon emissions. The stochastic user equilibrium is computed through an iterative method. The methodology is implemented and applied to a realistic test case in Lyon (France). The dynamic TCS profiles result in 36% fewer carbon emissions than static TCS for the same congestion reduction of 19%. Besides, 94% of the travelers benefit from the TCS as their travel costs decrease in the case study.

Keywords: generalized bathtub; tradable credit scheme; mode choice; departure time

INTRODUCTION

Automotive congestion has been an issue for many cities worldwide for decades. The traffic engineering and transportation economics communities proposed different demand management approaches to foster demand shift to off-peak periods and sustainable transportation modes. Tradable Credit Scheme (TCS) is a quantity-based framework introducing a commodity for traveling: credits. The regulator issues and distributes credits to the travelers. Depending on the departure time and transportation mode, a traveler needs to spend credits to access the transportation network. The credits can be traded between travelers through a dedicated marketplace. The offer and demand for credits are linked to the travel times of the different travel alternatives. Thus, estimating the congestion over the scale of a city is essential. Also, the design of the TCS, especially the number of credits needed for the different travel options, is linked to the goals the regulator wants to achieve. The most used objective function is related to the economic aspect of the congestion: the total travel time or the total schedule cost. It represents the time and money lost due to congestion. Other objectives linked to the environmental footprint of the transportation network, like the emissions of pollutants, can also be considered. However, reducing congestion or pollution might lead to different TCS, and trade-offs must be found. In this context, our contribution proposes a complete modeling framework to look for the optimal credit charging profile to minimize a given global objective considering the network equilibrium equilibration process. We proceed with a literature review on traffic congestion models and multimodality in TCS frameworks.

Congestion models

The problem of peak-hour congestion, i.e., when the travel demand exceeds the capacity for specific time periods, has been investigated for more than half a century (*1, 2*). The most common model in the literature of macroscopic traffic models is *Vickrey's bottleneck*. (*3*) represented the congestion as a point queue with a fixed capacity. The queue disappears by implementing marginal cost pricing, and the total schedule cost is reduced by a factor of two. In 1991, Vickrey relaxed the fixed capacity assumption (*4*) (work published posthumously) with a new model, named the *classical bathtub model*. The main idea is to define the network as an undifferentiated movement area with a mean speed function. The mean speed is defined as a function of network density and the network characteristics (*5, 6*). Therefore, the network speed decreases as the demand increases. (*7*) extended the framework to account for different desired arrival times. (*8*) proposed a numerical framework for determining the departure times distribution. (*9, 10*) introduced the trip-based Macroscopic Fundamental Diagram (MFD) to consider any trip length distribution. The mean speed is a function of vehicle accumulation, which is the key state variable of the classical bathtub and MFD models. (*11*) describes a numerical resolution method to compute the departure times distribution at equilibrium. (*12*) introduces an extension for the classical bathtub model, named *generalized bathtub*. The author presents a numerical framework for computing the travel times. The key state variable is the distribution of the remaining trip lengths of the travelers, which has also been introduced in (*11*). However, the departure times optimization is not addressed. Recently, (*13*) applied the Mean Field Game theory to compute the deterministic user equilibrium, and (*14*) computes the Stochastic User Equilibrium (SUE) for the generalized bathtub model. In this work, we use this modeling framework to capture the traffic dynamics and calculate the SUE.

Multimodality

Considering different transportation modes requires integrating different vehicle types into the road network. Multimodal macroscopic congestion models consider different travel times for the different vehicles and their interactions, especially between personal cars and buses. We can distinguish different approaches to represent multimodality in the literature: (i) the speeds for buses and cars are the same, and the bus dwelling time is explicitly considered (*15*); (ii) the bus speed is affine in the car speed (*16, 17*); (iii) modes other than the private car undergo an additional delay depending on the congestion level (*18*); (iv) each mode has its speed function, which is affine in the accumulation of every mode in the system (*19*). In this work, we use the second approach to capture the impact of car congestion on PT without adding too much complexity and calibration requirements.

Considering different vehicles may not be enough to account for the diversity of the mobility offer, especially with the rise of ride-hailing and -sharing services. A passenger car offers two different transportation alternatives if driven alone or used for carpooling. Some recent contributions in the literature (*20–23*) promoted carpooling to foster more sustainable travel behavior by reducing the number of driving vehicles. In the general framework, two travelers with similar trips would use only one car instead of two cars. On the one hand, users can drive on the High Occupancy Vehicle (HOV) lane, and the travelers share the expenses: fuel, congestion pricing, or credit/permit purchase. On the other hand, carpooling induces a penalty representing the detour and waiting time or the discomfort of not driving alone. This work aims at integrating time-dependent TCS, congestion dynamics, and multimodality, including carpooling, into a single framework.

TCS models in urban areas

A substantial part of the literature on TCS aims to optimize the travelers' route choices by charging the links of the networks, e.g., (*24*). Implementation of those contributions in an urban area is practically complex. The present work focuses on mode and departure time choices at the network level. Most studies in the literature used *Vickrey's bottleneck* model to address TCS at the network level to reduce the congestion (*25–30*). Besides (*31*) considered *Chu's model* (*32*) which is based on the BPR function. In the mentioned studies, the credit charge is dynamic, meaning the number of credits required to pass the bottleneck is time-dependent (i.e., based on the departure time choice). The purpose is to encourage travelers to switch from on-peak to off-peak hours. However, most of them only consider a single transportation mode with a homogeneous traveler's profile. (*26, 28, 30*) accounted for different Values of Time (VoT) to represent the heterogeneity of monetary valuation of the travel time for the personal car with Vickrey's bottleneck.

In our previous study, we proposed a TCS based on the trip-based MFD to capture trip heterogeneity (trip length) and congestion dynamics at a large scale (*33*). We considered Public Transportation (PT) with fixed cost based on a given departure time and origin-destination locations. The credit charge was static, i.e., the required number of credits does not depend on the departure time, as the focus is the shift from personal cars to PT. Recently, (*34*) also used trip-based MFD as well without PT, while the dynamic credit charge is designed proportionally to the travel distance. In this work, the TCS is dynamic and depends on the users' departure time and mode (private car, PT, and carpooling) choices. In addition, we consider a multimodal extension of the generalized bathtub model (*12*) to address the network equilibrium with a heterogeneous demand profile and to investigate the effect of a TCS on mode and departure time choices.

Moreover, we take into account environmental measures (CO2 emissions) not only to evaluate the performance of TCS but also to optimize the dynamic charging profile. In the literature,

there are few studies that consider environmental goals with TCS (*35*). To highlight our contributions, we compare the most relevant studies on TCS at the network level, including the departure time choice problem in Tab. 1, along with our previous work on MFD under TCS. This study addresses the gap between realistic congestion representation and dynamic TCS. Recall that dynamic TCS means that the credit charge may change depending on the time. The time- and mode-dependent TCS aims to foster mode and departure times shift to mitigate congestion and reduce the carbon footprint of the transportation network. We consider three travel modes: personal car, PT, and carpooling.

TABLE 1: Comparison of the different contributions on TCS

Article	Congestion model	Travel choice	Different VoT	Charging scheme	Pollution
(*25*)	Vickrey	Departure time and elastic demand	No	Dynamic	No
(*26*)	Vickrey	Mode and departure time	Yes	Dynamic	No
(*27*)	Vickrey	Departure time	No	Dynamic	No
(*28*)	Vickrey	Departure time	Yes	Dynamic	No
(*29*)	Vickrey	Departure time	No	Dynamic	No
(*30*)	Vickrey	Departure time	Yes	Dynamic	No
(*31*)	Vickrey / Chu	Departure time	No	Dynamic	No
(*34*)	Trip-based MFD	Departure time	Yes	Dynamic and distance-based	No
(*33*)	Trip-based MFD	Mode	No	Static	Yes
This work	Multimodal generalized bathtub	Mode and departure time	Yes	Dynamic	Yes

The remainder of this paper is organized as follows. In Sect. 2, we present the multimodal generalized bathtub framework with the TCS. Sect. 3 formulates the computation of the SUE under a dynamic TCS. The case study and the associated results are presented in Sect. 4 for a realistic morning commute in Lyon (France). Sect. 5 concludes this paper.

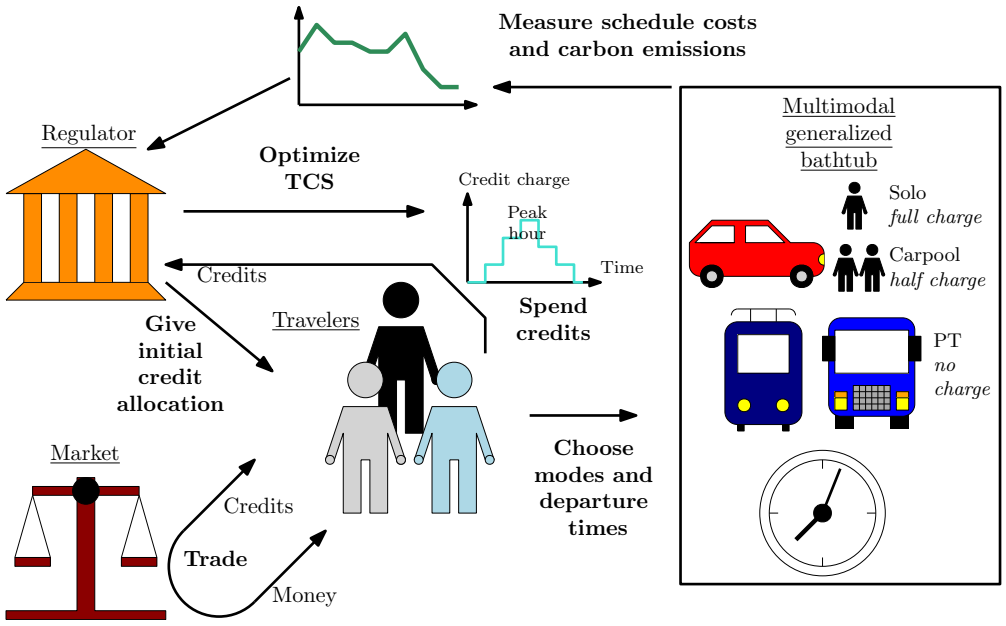

FIGURE 1: Framework of the multimodal bathtub under TCS.

PROBLEM FORMULATION

This section describes the proposed modeling framework to represent the TCS problem, including the SUE calculation based on the multimodal generalized bathtub under TCS. Fig. 1 depicts an overview of the different components and interactions in our framework. In Fig. 1, the travelers get a fixed amount of credits daily from the regulator. Obviously, this amount is insufficient to travel by car during peak hours. Otherwise, the TCS would be pointless. Travelers can trade the credits on a specific market. They choose their transportation mode and departure time according to the credit charging profiles and scheduling preferences. The regulator determines the credit charging profile to achieve its economic and environmental goals. The related measures (e.g., total travel time and carbon emissions) depend on the travelers' behaviors. The credit price results from the offer (supply) and demand in this market, so it depends on the travelers' choices. Thus, there are complex interdependencies between travelers' choices, the market, and the traffic congestion level. While describing credit price evolution during the transitional phase is very challenging, it is possible to calculate the credit price at equilibrium when all interactions stabilize. The next subsection presents the congestion model based on the generalized bathtub. Then the TCS is presented with a dynamic charging profile. Finally, we present the user choice model and the SUE formulation.

Multimodal generalized bathtub

Here we introduce the concepts, assumptions, and notations related to the congestion model. In this framework (see Fig. 1), travelers have different characteristics: trip length $l \in \mathscr{L}$, desired arrival time, $t_a \in \mathscr{T}_a$, and scheduling preferences α_c, $\tilde{\beta}_c$, and $\tilde{\gamma}_c$ associated to their socioeconomic class $c \in \mathscr{C}$. The capital and curly letter represents the domain of validity of the respective parameter or variable. They choose their departure times $t_d \in \mathscr{T}_d$ and travel modes $m \in \mathscr{M}$ according to the corresponding travel costs. The overall travel demand is described by the distribution $d = d(c,l,t_a)$. The total number of travelers is denoted by D. A demand scenario (the result of traffic assignment)

is represented by distribution $f = f(c,l,t_a,t_d,m)$. In this paper, we consider three transportation modes: car solo (one traveler per car), carpooling (two travelers per car), and public transportation (PT). ζ_m is the waiting time linked to mode m. We set it to zero for the solo car drivers and PT riders. It represents the extra time related to carpooling (waiting and small detour time) in this paper. We make no distinction between driver and passenger for carpooling: both have the same travel time and credit charge. It means the driver waits at the origin, and its waiting time in the car is equivalent to the passenger walking time to the driver's origin during ζ_{pool}. Then both start their trips.

The travel cost of mode m is calculated based on the arrival time obtained by bathtub dynamics equations. This congestion model assumes all trips take place in the same urban region, where the speed is spatially uniform. The mean speed for a given time is a function of the number of vehicles (personal cars, buses, tramways) circulating in the network at this time. A vehicle enters the network at the departure time t_d and leaves it once it has driven its trip length l. The generalized bathtub model provides a set of equations per transport mode. For each mode m, we define a virtual traveler $t \mapsto z_m(t)$ which keeps track of the cumulative traveled distance since the origin of times, as introduced by (*11*) (a.k.a. characteristic travel distance in (*12*)). We also define $H_m(t)$ as the accumulation, i.e., the number of vehicles of type m in the network at time t. The number of active trips with remaining distance higher than x at t is denoted $k_m(x,t)$. This state variable is specific to the generalized bathtub. The accumulation is then computed by $H_m(t) = k_m(x = 0,t)$. Recall that the accumulation is a state variable common to both MFD and bathtub representations. The speed of mode m v_m depends on the accumulations of all modes (*16–19, 36*). The coupling between the modes in the bathtub model occurs through the speed functions.

The accumulation at time t consists of the trips that started before t and are long enough to be ongoing by t. Therefore, we introduce the density, with respect to departure time t_d, of the number of vehicles with trip length longer than l: $F_m(l,t_d)\,\mathrm{d}t_d$. The traffic dynamics are based on the formulation of (*13*) and extended here to account for different modes. The bathtub dynamics of mode $m \in \mathscr{M}$ is given by Eq. 1.

$$\begin{cases} z_m(t) & = \int_0^t v_m(\{H_{m'}(s)\}_{m' \in \mathscr{M}})\mathrm{d}s \\ H_m(t) & = \int_0^t F_m(z_m(t) - z_m(t_d), t_d)\mathrm{d}t_d \\ F_m(l,t_d) & = \int_{l' > l, l' \in \mathscr{L}} \int_{t_a \in \mathscr{T}_a} \sum_{c \in \mathscr{C}} f(c,l',t_a,t_d,m)\mathrm{d}l'\mathrm{d}t_a \end{cases} \tag{1}$$

The first equation states that the mean speed depends on the accumulations and computes the trajectory of the virtual traveler $z_m(t)$. The second computes the accumulation $H_m(t)$: the sum of the trips that started earlier and are long enough to remain active. It depends on the trajectory of the virtual traveler $z_m(t)$. The third equation is the computation of the density $F_m(l,t_d)$ based on the traffic assignment f. The natural setting for the solutions of Eq. (1) is the space of Lipschitz continuous functions of time. In this space, it can be shown that given a distribution f, the solution (z_m, H_m) of Eq. (1) exists, is unique, and depends continuously on f for the weak topology of bounded measures. This follows by adapting propositions 1 to 4 and their proofs (appendices B to E) in (*13*).

The arrival time $\hat{t}_a$ is computed by using the inverse of the virtual traveler $x \mapsto z_m^{-1}(x)$. The inverse is correctly defined as long as the mode speeds are always non-zero. We assume the mean speeds are always strictly positive, meaning we exclude the possibility of a complete gridlock. A user starting at t_d with trip of length l and using mode m will arrive at

$$\hat{t}_a = t_d + z_m^{-1}(z_m(t_d) + l) + \zeta_m. \tag{2}$$

If the mode speeds are bounded from below, it can be shown that $\hat{t}_a$ depends continuously on (l, t_d) and that the function $(l, t_d) \mapsto \hat{t}_a$ depends continuously on f for the weak topology of bounded measures. This result follows by adapting proposition 5 and its proof (appendix G) in (*13*). To address the realistic demand profile based on trip data, we use the discretization approach to represent the formulation of the multimodal generalized bathtub to compute the arrival times via the trajectory of the virtual traveler z_m and the accumulation H_m, which are inter-dependent.

Discretization

The discretization approach aims to compute the arrival times of the multimodal generalized bathtub (Eq. (1)) in uniform intervals. Note that the discretization is not applied in our previous study, (*33*), since we used a more advanced trip-based MFD simulation framework, wherein the arrival times are computed following an event-based simulation: the state variables are updated each time a vehicle enters or leaves the network. The equilibrium computation was based on the linearization of the travel times with respect to the mode choices (*37*). This former approach is not suited here for the following reasons: (i) the travel time linearization while accounting for departure time becomes too complex as it adds another dimension to the problem; (ii) for each trip length, departure time, and mode, we would need one agent to account for the effect of this specific demand on the congestion. The computational cost of event-based resolution of the trip-based MFD increases quickly with the number of agents, as the state variables are updated each time an agent enters or leaves the network Idoudi et al. (*38*). To sum up, the main difference between the two approaches is that the trip-based MFD framework specifically follows each traveler and tracks its remaining travel distance. On the contrary, the generalized bathtub focuses on the distribution of the remaining trip lengths with fixed time steps. It is advantageous in terms of complexity and computation time to use the generalized bathtub framework, which is continuous. However, in a later section (4.4), we will simulate the optimal TCS solution with the more advanced trip-based MFD formulation to show that using the simplified approximation through the discretization of the generalized bathtub model in the optimization process makes perfect sense.

Since the solution is Lipschitz continuous, we approximate the solution $(z_m(t), H_m(t))$ as piece-wise linear functions calculated at nodal points. The numerical resolution of the bathtub requires the discretization of the trip length, departure time, and desired arrival times. The values of those discretized parameters and variables are identified by the following indexes:

$$\begin{cases} i_l = \lfloor (l - l_{\min})/\Delta_l + 0.5 \rfloor; \\ i_{t_d} = \lfloor t_d/\Delta_t + 0.5 \rfloor; \\ i_{t_a} = \lfloor (t_a - t_{a,\min})/\Delta_{t_a} + 0.5 \rfloor, \end{cases} \tag{3}$$

with $l_{\min}$ the minimum trip length and $t_{a,\min}$ the minimum desired departure time. $\lfloor x \rfloor$ is the integer part of x, i.e., the highest integer smaller than x. The first admissible departure time is taken as reference, i.e., is zero. The simulation time shares the same discretization as the departure times. One can come back to the continuous value of the variables from the indexes:

$$\begin{cases} l = l_{\min} + i_l \Delta_l; \\ t = i_t \Delta_t; \\ t_a = t_{a,\min} + i_{t_a} \Delta_{t_a}. \end{cases} \tag{4}$$

In the rest of the paper, we use both the discrete and continuous formulations for the arguments of the functions interchangeably. The discrete versions of the demand and the assignment are defined

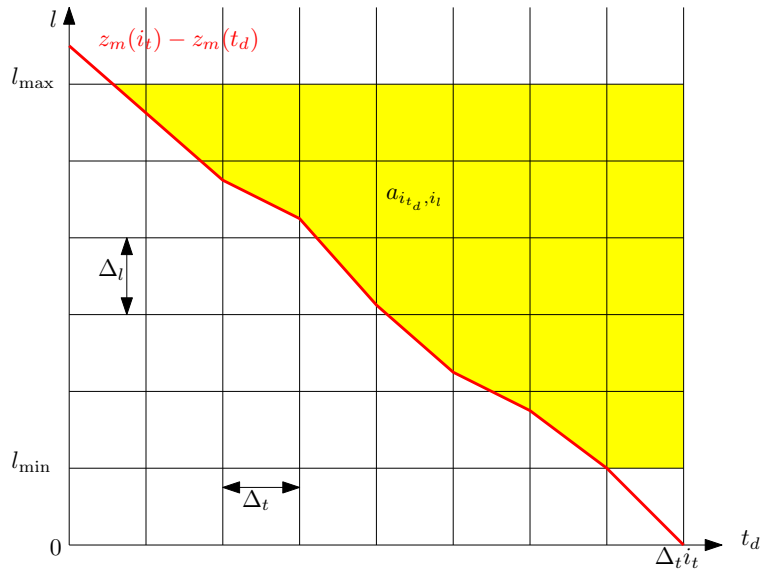

FIGURE 2: Discretization of the accumulation computation.

by:

$$\begin{cases} d(c,i_l,i_{t_a}) & = \int_{\Theta(i_{t_a})} \int_{\Theta(i_l)} d(c,l,t_a) \mathrm{d}t_a \mathrm{d}l; \\ f(c,i_l,i_{t_a},i_{t_d},m) & = \int_{\Theta(i_{t_a})} \int_{\Theta(i_l)} \int_{\Theta(i_{t_d})} f(c,l,t_a,t_d,m) \mathrm{d}t_a \mathrm{d}l \mathrm{d}t_d; \end{cases} \tag{5}$$

with

$$\begin{cases} \Theta(i_{t_a}) & = [t_{a,\min} + (i_{t_a} - 0.5)\Delta_{t_a}, t_{a,\min} + (i_{t_a} + 0.5)\Delta_{t_a}], \\ \Theta(i_l) & = [l_{\min} + (i_l - 0.5)\Delta_l, l_{\min} + (i_l + 0.5)\Delta_l], \\ \Theta(i_{t_d}) & = [(i_{t_d} - 0.5)\Delta_t, (i_{t_d} + 0.5)\Delta_t]. \end{cases} \tag{6}$$

The dynamics computation involves the resolution of Eq. (1) time step by step. The integration of the virtual traveler trajectory is straightforward: on each time step i_t, the traveled length z_m increased with the speed corresponding to the previous accumulation $H_m(i_{t-1})$ plus the trips starting in this step. The accumulation computation is represented by the yellow area in Fig. 2. Each square contributes to the accumulation at i_t with $a_{i_{t_d},i_l} \in [0,1]$ the ratio of the square above the line $t_d \mapsto z_m(i_t) - z_m(t_d)$ (i.e., the yellow part) multiplied by the number of trips starting at i_{t_d} with trip length i_l, $\sum_{c,i_{t_a}} f(c,i_l,i_{t_a},i_{t_d},m)$.

$$\begin{cases} z_m(i_t) & = z_m(i_{t-1}) + \Delta_t v_m \left(\{H_{m'}(i_{t-1}) + \sum_{c,i_{t_a},i_l} f(c,i_l,i_{t_a},i_t,m')\}_{m' \in \mathscr{M}} \right) \\ H_m(i_t) & = \sum_{i_{t_d} \leq i_t} F_m \left(\max(0, \lfloor \frac{(z_m(i_t) - z_m(i_{t_d}) - l_{\min})}{\Delta_l} \rfloor), i_{t_d} \right) \\ F_m(i_l,i_{t_d}) & = \sum_{i_{l'} \geq i_l} \sum_{c,i_{t_a}} a_{i_{t_d},i_{l'}} f(c,i_{l'},i_{t_a},i_{t_d},m) \end{cases} \tag{7}$$

Recall that F_m is a density with respect to t_d. $F_m(i_l,i_{t_d})$ is defined as the integral of $F_m(l,t_d)$ over $\Theta(i_{t_d})$. z_m and H_m are initialized with zero. The second part of the first equation allows us to account for the accumulation due to the trips starting during the current time step i_t. It counterbalances the fact that the bathtub tends to underestimate the congestion compared to the exact solution (computed via the trip-based MFD framework). Without this correction, the underestimation can be significant: with the case study, the equilibrium without TCS based on the generalized bathtub corresponds to gridlock with the exact solution (trip-based MFD).

Dynamic Tradable Credit Scheme

Some mobility alternatives require credits depending on the transportation mode m and departure time t_d. The credit charge is significant for highly congestive modes like private cars during peak hours and low for more sustainable choices like PT or carpooling outside peak hours. The regulator should set the charging profile $\tau(t_d, m)$ according to congestion and carbon emissions goals. In the following, the regulator only chooses the profile for car drivers $\tau(t_d, \text{car})$. It is free for PT riders: $\tau(t_d, \text{PT}) = 0$ and only the half for carpoolers as we assume two travelers per car: $\tau(t_d, \text{pool}) = \frac{1}{2}\tau(t_d, \text{car})$. Travelers receive a free initial allocation of κ credits from the regulator. They can trade the credits between themselves in a dedicated market. The credit price p is not fixed by the regulator. It is determined by the law of offer and demand in the market. We do not consider the details of the trade mechanism. We adopt the widely used Market Clearing Condition (MCC), as in (*24*), to represent the market mechanism: the price is zero or all issued credits are spent.

Mode and departure time choice

The travel time (TT) of a traveller leaving at t_d and arriving at $\hat{t}_a$ is

$$TT = \hat{t}_a - t_d. \tag{8}$$

The schedule cost (SC) accounts for the early or late arrival on top of the TT. The SC of a traveler of the class c with the desired arrival time t_a finishing its trip at $\hat{t}_a$ is

$$SC = \alpha_c \left((\hat{t}_a - t_d) + \tilde{\beta}_c \max(0, t_a - \hat{t}_a) + \tilde{\gamma}_c \max(0, \hat{t}_a - t_a) \right). \tag{9}$$

$\alpha_c, \tilde{\beta}_c$, and $\tilde{\gamma}_c$ are respectively the VoT and the normalized marginal cost for early and late arrival. The travel cost (TC) is obtained by adding the TCS-related cost, i.e., the monetary value of the required credits:

$$TC = SC + p\tau(t_d, m). \tag{10}$$

Both SC and TC depend on trip length, departure time, mode, desired arrival time, and class. However, we do not make it explicit in the equations to keep the notations light. The discrete logit-based decision depends on the TC of all alternatives regarding departure time and mode choice, and on the logit parameter θ_c:

$$\psi(c, i_l, i_{t_a}, i_{t_d}, m) = \frac{e^{-\theta_c TC(c, i_l, i_{t_a}, i_{t_d}, m)}}{\sum_{i_{t'_d}, m'} e^{-\theta_c TC(c, i_l, i_{t_a}, i_{t'_d}, m')}}. \tag{11}$$

$\psi(c, i_l, i_{t_a}, i_{t_d}, m)$ is the ratio of travelers with characteristics c, i_l, i_{t_a} *wanting* to travel at t_d with mode m. It may be different from the *actual* travel assignment $f(c, i_l, i_{t_a}, i_{t_d}, m)/d(c, i_l, i_{t_a})$.

Equilibrium formulation

The SUE formulation is based on (*14*). It is extended to account for the mode choice and the TCS constraints. The SUE is reached when the flow distribution matches the logit distribution:

$$d(\omega)\psi(\omega) = f(\omega) \;\forall\; \omega \in \Omega, \tag{12}$$

with $\Omega = \mathscr{C} \times \mathscr{L} \times \mathscr{T}_a \times \mathscr{T}_d \times \mathscr{M}$ the space of all travelers' characteristics and degrees of freedom. The flow conservation requires the travel demand with specific characteristics to match the sum of the flows with the same characteristics:

$$\sum_{i_{t_d}, m} f(c, i_l, i_{t_a}, i_{t_d}, m) = d(c, i_l, i_{t_a}) \;\forall\; c, i_l, i_{t_a}. \tag{13}$$

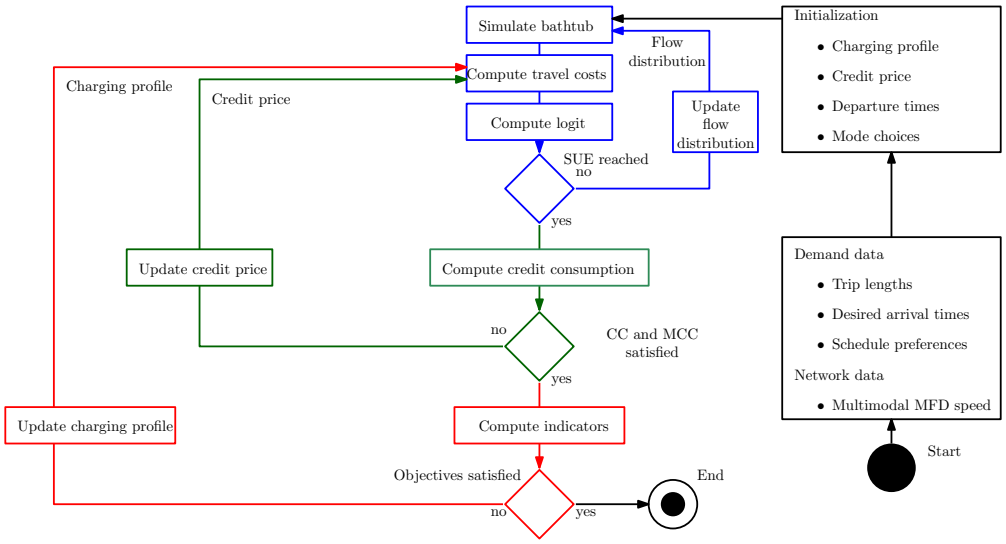

FIGURE 3: Algorithm flowchart.

The TCS-specific constraints are respectively the credit cap (CC): the consumed credits cannot exceed the allocated amount, the MCC, and the positivity of the price:

$$\begin{cases} \sum_{\omega\in\Omega} f(\omega)\tau(\omega) \leq D\kappa; \\ \left(\sum_{\omega\in\Omega} f(\omega)\tau(\omega) - D\kappa\right) p = 0; \\ p \geq 0. \end{cases} \tag{14}$$

METHODOLOGICAL FRAMEWORK

The equilibration of the multimodal generalized bathtub model under TCS is decomposed into two imbricated loops. Basically, the outer loop increases (respectively decreases) the price if too many (too few) credits are consumed until the MCC and CC hold: (i) price is zero and some credits are not used, or (ii) all credits are consumed. The inner loop changes the travelers' departure times and travel modes until their logit-based decisions match their actual travel assignments. The two loops form two imbricated fixed-part problems to be solved. Fig. 3 presents the two loops: blue for the assignment and green for the credit price. The red one indicates the optimization of the charging profile. This optimization process is adapted based on our previous study (*33*). The idea of charging profile optimization is presented in (*33*). Here, we only describe credit price evolution and SUE calculation.

Credit price

We define the credit consumption excess R as

$$R = \frac{1}{D} \sum_{\omega\in\Omega} f(\omega) \left(\frac{\tau(\omega)}{\kappa} - 1 \right). \tag{15}$$

It is the normalized number of credits used minus the initial allocation. The CC dictates it should be negative: we accept unused credits but not the consumption of non-existing ones. The CC error is defined as the positive part of R:

$$E_{\mathrm{CC}} = \max(0, R). \tag{16}$$

The MCC error is defined as

$$E_{\text{MCC}} = p\kappa|R|. \tag{17}$$

It is high when the price is non-zero and all credits are not consumed. We use the absolute value of R to ensure a positive metric for the MCC error.

We change the credit price if one of the error measures E_{CC} or E_{MCC} is higher than the given respective thresholds E^*_{CC} and E^*_{MCC}. The price variation of the CC and MCC loop for the iteration $i_{\text{step,pri}}$ of the price loop is

$$\Delta p = \frac{1}{\sqrt{i_{\text{step,pri}}}} \frac{1}{\kappa} R. \tag{18}$$

The amplitude of the change decreases as the loop iterates to force convergence but not too fast to allow for space exploration. We bound Δp by $\pm\varepsilon_p$, a fixed threshold to prevent large oscillations. The price is then updated, by ensuring it stays positive:

$$p = \max(p + \Delta p, 0). \tag{19}$$

The price loop iterates until the maximum number of iterations is reached, or both CC and MCC errors fall below the given thresholds.

Assignment

The SUE error quantifies the difference between assignment and logit-based decision:

$$E_{\text{SUE}} = \frac{1}{D} \sum_{\omega \in \Omega} |f(\omega) - d(\omega)\psi(\omega)|. \tag{20}$$

The assignment loop starts with an initial solution based on free flow mean speed and then iterates until the maximum number of iterations is reached or the SUE error falls below a threshold E^*_{SUE}. A heuristic reassignment algorithm is designed to correct the worst decisions (assignment far from logit) with a procedure similar to the MSA. We first rank the assignment based on the SUE error. Then, we choose the proportion of the assignments with larger errors and reassign their departure time and mode choice. This procedure is inspired from (*39*). The proportion corresponds to the step size of the algorithm. A search index is defined and initialized with $r = 1$. For each iteration of the SUE loop, the fraction $1/r$ of the assignment characteristics $\omega \in \Omega$ where the assignment error $|f(\omega)/d(\omega) - \psi(\omega)|$ is the largest is updated. We name this part of the travel characteristics $\mathscr{F}$. The rest of the characteristics define the ensemble $\bar{\mathscr{F}}$. Thus $\mathscr{F} \cup \bar{\mathscr{F}} = \Omega$ and $\mathscr{F} \cap \bar{\mathscr{F}} = \varnothing$. The step size formulation is the same as the step size of the MSA method; however, we use the smart step size approach (*40*) to update the step size for the following iterations. If the new flow distribution leads to a smaller SUE error E_{SUE}, then the search index stays the same. Otherwise, the search index r increases by one, decreasing the search radius. The convergence of this approach is discussed in (*41*). We stop once the SUE error falls below a given threshold, or the best solution (lowest SUE error) is returned if the maximum number of iterations is reached.

NUMERICAL EXPERIMENTS

Case Study

The travel demand considered for the case study represents the typical morning commute of 384,200 travelers in Lyon (France) between 7:00 and 10:00. There are ten regions and five boundaries, creating 224 different OD-pairs with non-zero demand Alisoltani et al., Alisoltani et al. (*42*, *43*). The travel demand consists of trips in Lyon and also trips through Lyon, i.e., we also account for travelers starting or/and ending their trip outside the city Amelia et al. (*44*). Fig. 4(a) represents the studied network. The synthetic desired arrival times are shown in Fig. 4(b). The

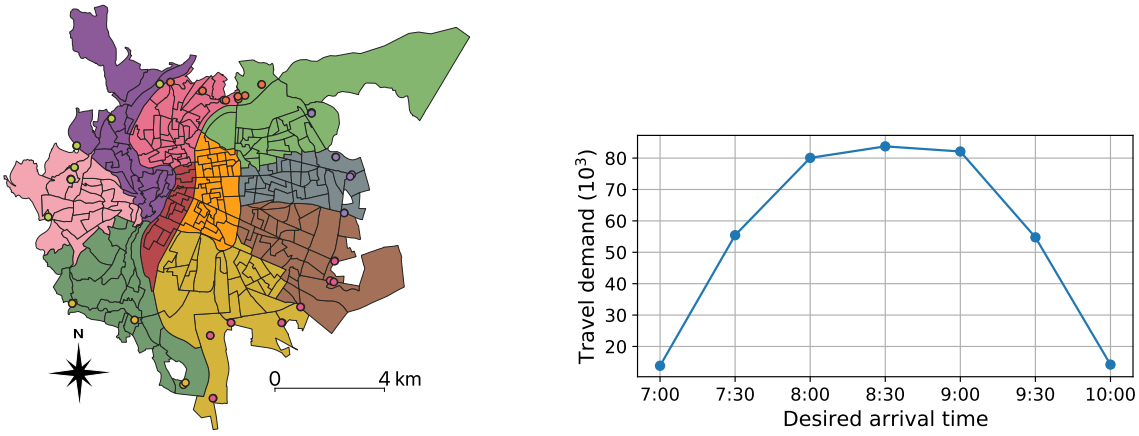

(a) (b)

FIGURE 4: Supply and demand for the scenario: (a) the ten regions formed by the IRIS areas and the access points merged in five boundaries (circles) (b) and the distribution of the desired arrival times.

distribution has a bell shape: the demand is low at 7:00 and 10:00 and high between 8:00 and 9:00 Ameli et al. (*45*).

An MFD speed function represents the network capacity. All trips occur in the same region. The mean speed depends only on the car accumulation (solo drivers and carpoolers). We assume the number of operating buses is given and thus already accounted for in the speed function. The speed function does not depend explicitly on the accumulation of buses. We calibrated the affine formulation from (*16, 46*) with the travel times and distances retrieved from the city navigator (*47*). The travel demand acts as the weighting factor. The PT speed is assumed affine in the car speed. It is computed by (numerical values for speed in m/s):

$$V_{\mathrm{PT}} = 0.12 V_{\mathrm{car}} \left(H_{\mathrm{car}} + \frac{1}{2} H_{\mathrm{pool}} \right) + 3.17. \tag{21}$$

Note that the constant factor is higher and the proportionality factor lower than in (*16*). In the former study, the authors represented the speed of buses only, whereas we consider tramways and subways as well. Those modes are not or very little impacted by the car congestion Ameli et al. (*48*).

The trip length is discretized with 50 steps (precision of 304 m) and the departure time with 100 steps (precision of 145 s). We assume seven possible desired arrival times: every 30 min from 7:00 to 10:00. Those numerical values are chosen as a trade-off between computation times, numerical rounding errors, and simulation precision. To account for the equity of the TCS concerning the travelers' wealth, we consider travelers with a low VoT of 10.8 EUR/h for low revenue and a high VoT of 21.6 EUR/h to represent high revenue. We assume there are evenly distributed across the travel demand. These VoT correspond to the order of magnitude of Lyon inhabitants' VoT distribution, as used in (*49, 50*). The normalized early factor is chosen as 1/2 and the late one as 2. It represents that being late is worse than traveling a long time, which is worse than arriving early. It is a common assumption when computing schedule cost as a proxy for the perceived travel cost. This choice of discretization leads to 210,000 different combinations of travelers' characteristics and trip choices: 50 trip lengths, 100 departure times, seven desired arrival times, two VoT,

and three modes. The trip-based MFD (event-based resolution) solution is expensive to compute for such a large set of trips. One simulation lasts about 470 s with the trip-based MFD and only 0.1 s with the generalized bathtub. The trip-based framework is only used to confirm that the generalized bathtub approximation provides a close approximation of the system states for the optimal solution.

We estimate the carpooling penalty ζ_{pool} with additional 10 min. The main parameters used for the numerical computation are gathered in Tab. 2. Note that the allocation κ is only meaningful compared to the charging profile τ, as only the ratio matters.

TABLE 2: The parameters used for the simulation.

Parameter	Notation	Value
VoT	α_c	$\{10.8, 21.6\}$ EUR/h
Scaled early factor	$\tilde{\beta}$	1/2
Scaled late factor	$\tilde{\gamma}$	2
Endowment	κ	1 credit
SUE goal	E^*_{SUE}	10^{-2}
CC goal	E^*_{CC}	5×10^{-3}
MCC goal	E^*_{MCC}	5×10^{-3}
Maximum price variation	ε_p	1 EUR
Logit parameter	θ_c	1 1/EUR
Carpooling penalty	ζ_{pool}	10 min
Charging period	T_{charges}	30 min

The charging period is chosen based on the travel times distribution without TCS. The credit charge changes every 30 min, and most of the trips (about 90%) last less than this period. It means most of the trips finish at most in the period after which they started. It is essential not to have too many trips impacting a large number of periods, as these travelers would impact the traffic conditions without paying the appropriate charge. It goes in the sense of marginal cost pricing: the traveler pays for the externality that it causes to the rest of the travelers.

Results at the network level

We generate different dynamic TCS forming a Pareto front, i.e., the ones with no other solution being better at the same time for congestion and carbon emission reduction. The carbon emissions are estimated using the COPERT IV (*51*) model of (*52*). We also compute the equilibrium under static credit charging, with different ratios charge over allocation $\tau(\text{car})/\kappa$ between 3 and 16. The Pareto front is shown in Fig. 5, with the static solutions and the no TCS case for comparison. A static charge of 4 credits means that, on average, only one car can drive for every four travelers (one solo driver or two carpoolers). It already enables a congestion reduction of about 19% and pollution of 59%. To achieve a low carbon footprint, the TCS greatly penalizes the car, and many travelers switch to PT and carpooling. The mode shift is large, the traffic improvement does not offset the use of slower modes, and the total congestion cost increases due to increased travel times. The congestion cost reduction of 20% (dynamic charging 'cong') cannot be reached with static charging. Even if static charging enables a congestion reduction of 19%, the associated carbon emissions are 36% higher than the dynamic TCS 'cong'. We keep the dynamic solutions with

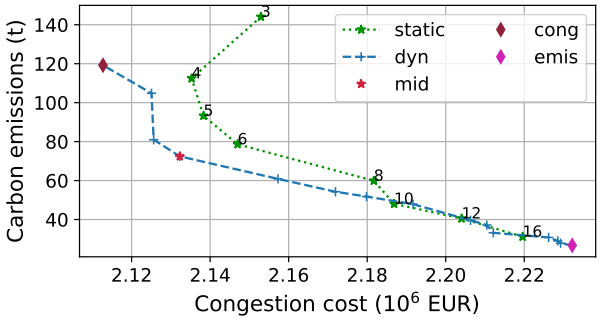

FIGURE 5: Congestion cost vs. carbon emissions for different static and dynamic TCS. The numbers are the ratios charge over allocation for the static cases. For comparison, the no TCS case leads to a congestion cost of 2.63×10^6EUR and a carbon emission of 275 t.

the lowest congestion cost ('cong') and the lowest CO2 emission ('emis') for further comparison against static charging. An intermediate case of dynamic charging ('mid') is used for comparison against the no TCS scenario.

We compare the modal shares for the different scenarios in Fig. 6. As expected, we see from Fig. 6(a) that the share of solo drivers diminishes with TCS as the associated travel costs increases. Looking more closely reveals the car share decreases with dynamic charging during the peak demand, while it increases with static charging. There are two effects to explain this: it becomes expensive to take the car as the credit charge is high during the peak in the dynamic case. The credit charge is the same in the static case, but the travel demand is higher. The TCS 'cong' strongly reduces car share for a limited time (8:00 to 9:00), while the TCS 'emis' creates a substantial reduction across the whole time frame to reach ambitious pollution targets. The PT share (Fig. 6(b)) increases with the charging profile as it requires no credits. The share of carpoolers is captured in Fig. 6(c). The carpooling mode is more used with TCS than without TCS. However, the carpooling share decreases with the charging profile when the credit charge is high, as a carpooler still needs to spend credits. When looking at the shares with respect to the charging slots for all modes in Fig. 6(d), the TCS seems to make travelers leave later. The traffic conditions are improved, the travel times decrease, and thus travelers start their trip later to arrive around their desired arrival time. There is, however, very little difference between the different TCS. The conclusion is that the TCS affects the mode choice more than it affects the departure time distribution.

In Fig. 7, the traffic conditions with and without TCS are compared through the mean speeds. Without TCS, the mean speeds of PT and car (represented in Fig. 7(a)) are similar during the peak of the demand. As expected, the TCS improves the traffic conditions by reducing the number of circulating cars. The gain is considerable for cars, which circulate about 6 m/s (about 20 km/h) faster during the peak. The PT speed increases by about 1 m/s (about 4 km/h). The waves come from the discretization of the desired arrival times. It creates some local demand peaks every half an hour. Fig. 7(b) compares car speed for different objectives. When focusing on congestion reduction, i.e., reducing the total schedule cost, the TCS still allows mean speed reductions of more than 3 m/s. Especially, the credit charge is low before 8:00, and the demand is already high; thus, the mean car speed is lower than after 8:00. The TCS designed for emission reduction keeps the mean speed around 11 m/s. It is expected as the emissions decrease with the mean car speed for

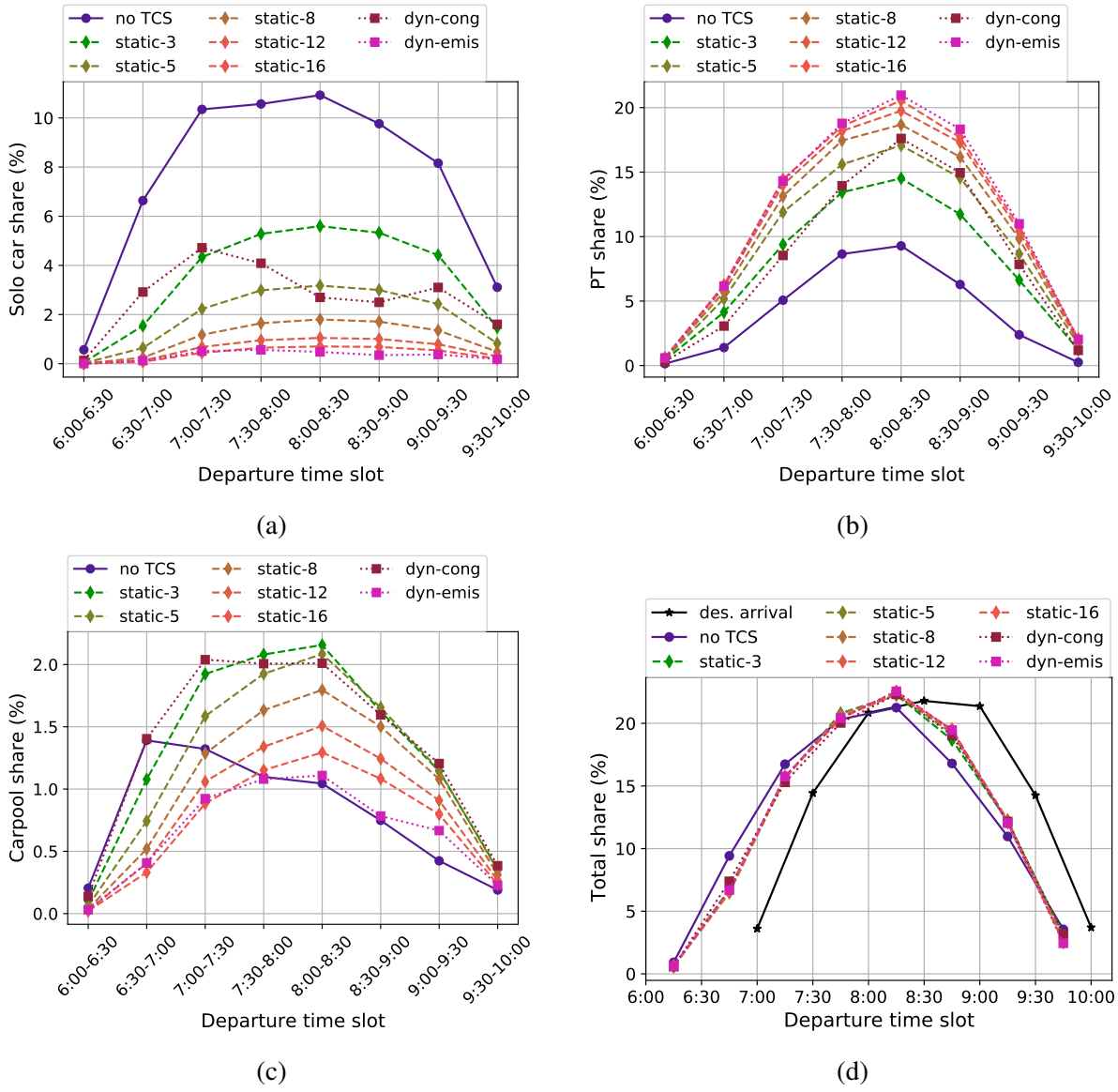

FIGURE 6: Evolution of the mode shares and the departure times for: (a) solo car, (b) PT, (c) carpool, and (d) total shares.

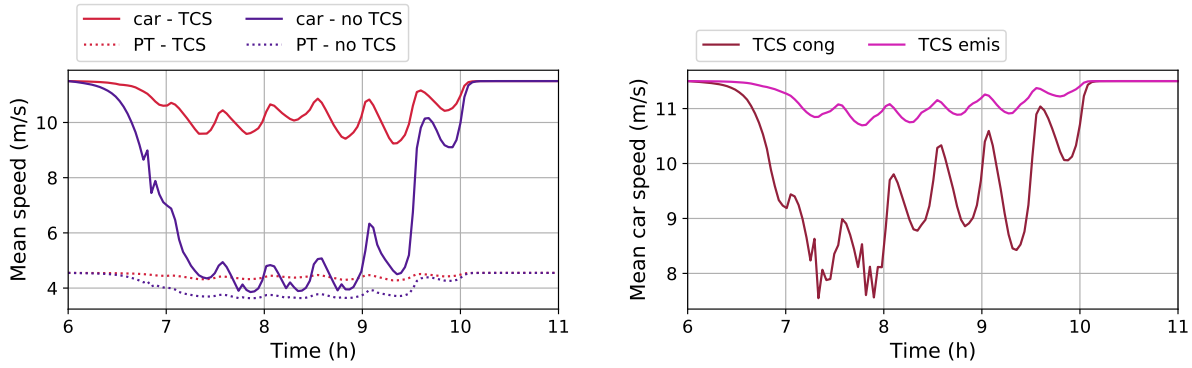

(a) (b)

FIGURE 7: Effect of the different dynamic TCS of the mean traffic speed: (a) mean car and PT speeds with dynamic TCS ('mid') and without TCS and (b) mean car speed for the TCS 'cong' and 'emis'.

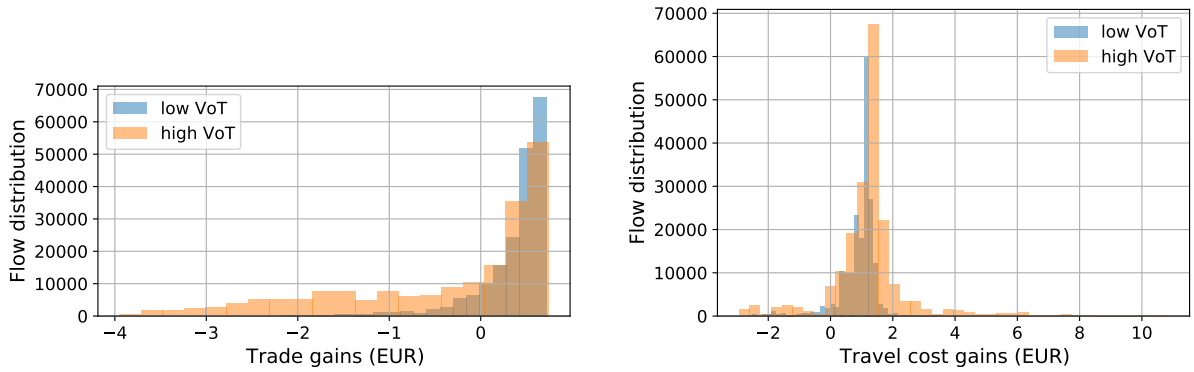

(a) (b)

FIGURE 8: Distribution of the benefits of the TCS: (a) trade gains (money earned or spent through the market) and (b) travel costs gains.

the range of urban speeds.

Individual gains

As we consider heterogeneous travelers in terms of desired arrival times, OD pairs, and VoT, it is crucial to look at the equity of the TCS. By looking at the distributions of the gains brought by the TCS ('mid'), we can quantify the number of travelers better off and worse off with the proposed policy.

The travel cost gain is the difference between travel costs without and with TCS. It is the sum of the schedule cost gain and trade gain from the market. A positive gain is favorable for the traveler as it means its cost decreases with the TCS. The trade gains from the market and the travel cost gains are represented in Fig. 8. A positive trade gain means the traveler earns money by selling credits while a negative gains means it spends money to buy credits. Fig. 8(a) gives an overview of the market outcomes. Travelers with a high VoT tend to buy credits from travelers with a smaller VoT; thus, they earn less money through the market. A traveler can earn around

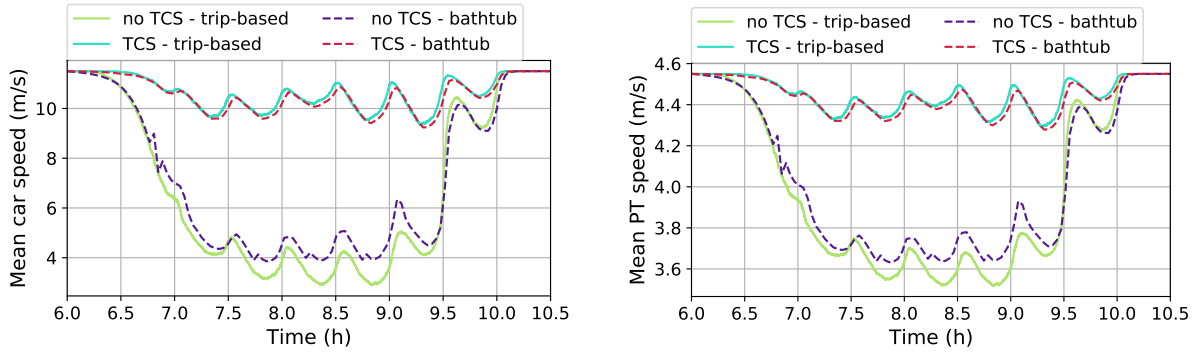

(a) (b)

FIGURE 9: Comparison of the mean speeds with and without TCS for the bathtub and trip-based MFD resolutions: (a) car and (b) PT.

0.8 EUR by riding PT and spend around 5.4 EUR driving its car alone during the highest charging period. When weighting the trade gains by the flow distribution, some travelers spend up to 4 EUR while others earn up to 0.7 EUR, depending on their characteristics (VoT, trip length, and desired arrival time). The effect of TCS on the travel cost (schedule cost plus credit trade) is represented in Fig. 8(b). Most travelers are better off with the TCS, as they decrease their travel costs by 0 to 2 EUR. About 6% of the travelers see their travel cost increase with this TCS, meaning 94% benefit from the TCS. The worst off lose 2.9 EUR, while those better off earn up to 10.8 EUR. Note that those estimations do not account for the benefits linked to the lower pollution levels, such as better air quality.

Comparison with the trip-based MFD

To assess the discretization effects, we compute the trip-based MFD simulation for the reference test case without TCS and the intermediate TCS 'mid'. The trip-based MFD, via its event-based resolution, provides the exact computation of the arrival times. It serves as the plant model. It does not use any discretization. It is, however, significantly more time-consuming to compute the arrival times for a given assignment than the discretization of the bathtub. Typically, the computation time is higher by three orders of magnitude. The trip lengths are the ones from the continuous demand before the discretization. The departure times are smooth: the trip linked to a departure time index i_{t_d} in the bathtub corresponds to a departure time randomly drawn from the uniform distribution $[(i_{t_d}-0.5)\Delta_t,(i_{t_d}+0.5)\Delta_t]$. We only consider trips with a flow higher than one traveler. Less than 2% of the travel demand is lost in the process. The mean car and PT speed are compared in Fig. 9. Some deviations, up to 1 m/s for car speed (Fig. 9(a)) and 0.1 m/s for PT speed (Fig. 9(b)), can be observed in the no TCS case between the network speed in the MFD and the bathtub. The differences are barely noticeable with TCS. The generalized bathtub tends to underestimate the congestion. To quantify the error made in congestion and pollution estimation with the bathtub, we compare the TCS and the carbon emissions both with and without TCS in Fig. 10.

The errors stay below 3% for congestion cost (Fig. 10(a)) and 11% for carbon emission (Fig. 10(b)). The numerical approximations of the multimodal generalized bathtub are below the differences between the scenarios with and without TCS. The numerical resolution of the bathtub still gives a reasonable quantification of the economic and environmental benefits of the TCS at a

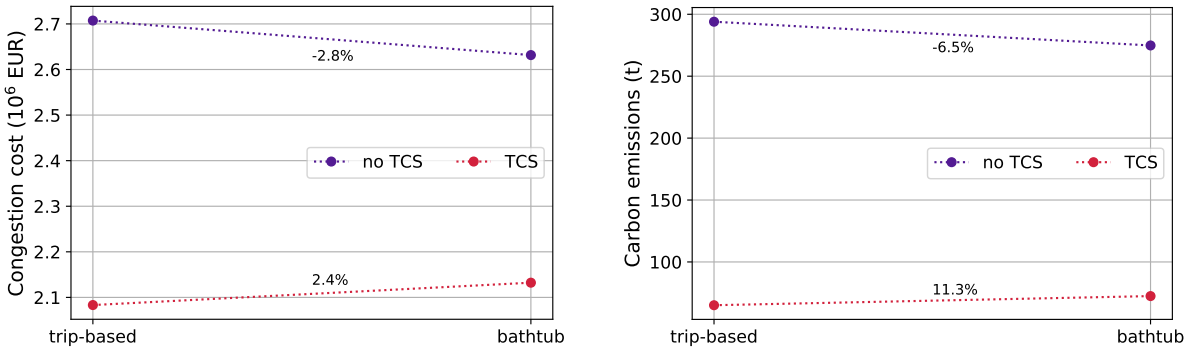

(a) (b)

FIGURE 10: Variations of the objectives measures between bathtub and trip-based MFD: (a) congestion cost (total schedule cost) and (b) carbon emission.

lower computational cost than the trip-based MFD.

CONCLUSION

During the last two decades, the literature improved the bottleneck's model to quantify better the economic losses caused by congestion. It also allowed us to understand better the potential benefits of demand management policies such as congestion pricing and Tradable Credit Scheme (TCS). The main mean of action was the spread of the departure times. We formulate a multimodal generalized bathtub to account for different types of vehicles and transportation modes with this work. Each traveler's choices consist of mode and departure time. We add a TCS to foster mode shift during the peak hour. Public Transportation (PT) users ride for free, solo car drivers pay the total charge, and carpoolers only half. We compute the Stochastic User Equilibrium (SUE) to account for the uncertainty of users' choices. A realistic scenario based on the morning commute in Lyon illustrates the proposed methodology.

The proposed framework makes it possible to compare the advantage of a dynamic TCS over a static one. The dynamic TCS accounts for the different demand levels depending on the time of the day. It permits a better reduction of the congestion costs, i.e., the sum of all travelers' schedule costs. The SUE is based on schedule cost; thus, the departure time shift of the travelers is relatively limited. The most considerable consequence is the mode shift: PT and carpooling mode shares increase at the expense of the car share. We draw a Pareto front to present how TCS can lead to different compromises in terms of congestion cost and carbon emissions.

As TCS is a policy involving the trade of credits, it raises the question of the individual gains when people have different VoT (different economic classes). The results show no significant disadvantage for one category of VoT. With the TCS, more than 94% of the population benefit from the TCS, as their travel costs are reduced with the TCS. Furthermore, It does not even account for the environmental aspects, like air quality. The numerical resolution of the multimodal generalized bathtub approximates the travel times. A comparison against the exact solution via trip-based MFD showed that the numerical error is below the order of benefits of the TCS. Moreover, the proposed methodology can efficiently assess and optimize the benefits of TCS. The framework uses the advantages of macroscopic simulation to limit the need for computation power and data collection requirement.

Further steps in the evaluation of dynamic TCS include the validation of the traffic simulation through micro-simulation and the estimation of travelers' behavior and acceptance through surveys.

ACKNOWLEDGEMENTS

This project has received funding from the European Union's Horizon 2020 research and innovation program under Grant Agreement no. 953783 (DIT4TraM).

REFERENCES

1. Li, Z. C., H. J. Huang, and H. Yang, Fifty years of the bottleneck model: A bibliometric review and future research directions. *Transportation Research Part B: Methodological*, Vol. 139, 2020, pp. 311–342.
2. Ameli, M., J.-P. Lebacque, and L. Leclercq, Improving traffic network performance with road banning strategy: A simulation approach comparing user equilibrium and system optimum. *Simulation Modelling Practice and Theory*, Vol. 99, 2020, p. 101995.
3. Vickrey, W. S., Congestion Theory and Transport Investment. *Source: The American Economic Review*, Vol. 59, No. 2, 1969, pp. 251–260.
4. Vickrey, W., Congestion in midtown Manhattan in relation to marginal cost pricing. *Economics of Transportation*, Vol. 21, 2020, p. 100152.
5. Fosgerau, M. and K. A. Small, Hypercongestion in downtown metropolis. *Journal of Urban Economics*, Vol. 76, No. 1, 2013, pp. 122–134.
6. Arnott, R., A bathtub model of downtown traffic congestion. *Journal of Urban Economics*, Vol. 76, No. 1, 2013, pp. 110–121.
7. Fosgerau, M., Congestion in the bathtub. *Economics of Transportation*, Vol. 4, 2015, pp. 241–255.
8. Arnott, R. and J. Buli, Solving for equilibrium in the basic bathtub model. *Transportation Research Part B: Methodological*, Vol. 109, 2018, pp. 150–175.
9. Mariotte, G., L. Leclercq, and J. A. Laval, Macroscopic urban dynamics: Analytical and numerical comparisons of existing models. *Transportation Research Part B: Methodological*, Vol. 101, 2017, pp. 245–267.
10. Leclercq, L., A. Sénécat, and G. Mariotte, Dynamic macroscopic simulation of on-street parking search: A trip-based approach. *Transportation Research Part B: Methodological*, Vol. 101, 2017, pp. 268–282.
11. Lamotte, R. and N. Geroliminis, The morning commute in urban areas with heterogeneous trip lengths. *Transportation Research Part B: Methodological*, Vol. 117, 2018, pp. 794–810.
12. Jin, W.-L., Generalized bathtub model of network trip flows. *Transportation Research Part B*, Vol. 136, 2020, pp. 138–157.
13. Ameli, M., M. S. S. Faradonbeh, J.-P. Lebacque, H. Abouee-Mehrizi, and L. Leclercq, Departure Time Choice Models in Urban Transportation Systems Based on Mean Field Games. *https://doi.org/10.1287/trsc.2022.1147*, 2022.
14. Lebacque, J.-P., M. Ameli, and L. Leclercq, Stochastic departure time user equilibrium with heterogeneous trip profile. In *The 10th symposium of the European Association for Research in Transportation (hEART)*, 2022.

15. Dakic, I., K. Yang, M. Menendez, and J. Y. Chow, On the design of an optimal flexible bus dispatching system with modular bus units: Using the three-dimensional macroscopic fundamental diagram. *Transportation Research Part B: Methodological*, Vol. 148, 2021, pp. 38–59.
16. Loder, A., L. Ambühl, M. Menendez, and K. W. Axhausen, Empirics of multi-modal traffic networks – Using the 3D macroscopic fundamental diagram. *Transportation Research Part C: Emerging Technologies*, Vol. 82, 2017, pp. 88–101.
17. Loder, A., I. Dakic, L. Bressan, L. Ambühl, M. C. Bliemer, M. Menendez, and K. W. Axhausen, Capturing network properties with a functional form for the multi-modal macroscopic fundamental diagram. *Transportation Research Part B: Methodological*, Vol. 129, 2019, pp. 1–19.
18. Loder, A., L. Bressan, M. J. Wierbos, H. Becker, A. Emmonds, M. Obee, V. L. Knoop, M. Menendez, and K. W. Axhausen, How Many Cars in the City Are Too Many? Towards Finding the Optimal Modal Split for a Multi-Modal Urban Road Network. *Frontiers in Future Transportation*, Vol. 0, 2021, p. 5.
19. Paipuri, M. and L. Leclercq, Bi-modal macroscopic traffic dynamics in a single region. *Transportation Research Part B: Methodological*, Vol. 133, 2020, pp. 257–290.
20. Xiao, L. L., T. L. Liu, and H. J. Huang, On the morning commute problem with carpooling behavior under parking space constraint. *Transportation Research Part B: Methodological*, Vol. 91, 2016, pp. 383–407.
21. Yu, X., V. A. van den Berg, and E. T. Verhoef, Carpooling with heterogeneous users in the bottleneck model. *Transportation Research Part B: Methodological*, Vol. 127, 2019, pp. 178–200.
22. Xiao, L. L., T. L. Liu, H. J. Huang, and R. Liu, Temporal-spatial allocation of bottleneck capacity for managing morning commute with carpool. *Transportation Research Part B: Methodological*, Vol. 143, 2021, pp. 177–200.
23. Xiao, L. L., T. L. Liu, and H. J. Huang, Tradable permit schemes for managing morning commute with carpool under parking space constraint. *Transportation*, Vol. 48, 2021, pp. 1563–1586.
24. Yang, H. and X. Wang, Managing network mobility with tradable credits. *Transportation Research Part B: Methodological*, Vol. 45, No. 3, 2011, pp. 580–594.
25. Nie, Y. M. and Y. Yin, Managing rush hour travel choices with tradable credit scheme. *Transportation Research Part B: Methodological*, Vol. 50, 2013, pp. 1–19.
26. Tian, L. J., H. Yang, and H. J. Huang, Tradable credit schemes for managing bottleneck congestion and modal split with heterogeneous users. *Transportation Research Part E: Logistics and Transportation Review*, Vol. 54, 2013, pp. 1–13.
27. Nie, Y. M., A New Tradable Credit Scheme for the Morning Commute Problem. *Networks and Spatial Economics*, Vol. 15, No. 3, 2015, pp. 719–741.
28. Xiao, L. L., H. J. Huang, and R. Liu, Tradable credit scheme for rush hour travel choice with heterogeneous commuters. *Advances in Mechanical Engineering*, Vol. 7, No. 10, 2015, p. 168781401561243.
29. Jia, Z., D. Z. Wang, and X. Cai, Traffic managements for household travels in congested morning commute. *Transportation Research Part E: Logistics and Transportation Review*, Vol. 91, 2016, pp. 173–189.

30. Miralinaghi, M., S. Peeta, X. He, and S. V. Ukkusuri, Managing morning commute congestion with a tradable credit scheme under commuter heterogeneity and market loss aversion behavior. *Transportmetrica B*, Vol. 7, No. 1, 2019, pp. 1780–1808.
31. Bao, Y., E. T. Verhoef, and P. Koster, Regulating dynamic congestion externalities with tradable credit schemes: Does a unique equilibrium exist? *Transportation Research Part B: Methodological*, Vol. 127, 2019, pp. 225–236.
32. Chu, X., Endogenous Trip Scheduling: The Henderson Approach Reformulated and Compared with the Vickrey Approach. *Journal of Urban Economics*, Vol. 37, No. 3, 1995, pp. 324–343.
33. Balzer, L. and L. Leclercq, Modal equilibrium of a tradable credit scheme with a trip-based MFD and logit-based decision-making. *Transportation Research Part C: Emerging Technologies*, Vol. 139, 2022, p. 103642.
34. Liu, R., S. Chen, Y. Jiang, R. Seshadri, M. Ben-Akiva, and C. L. Azevedo, Managing network congestion with a trip- and area-based tradable credit scheme. *Transportmetrica B: Transport Dynamics*, 2022, pp. 1–29.
35. Gao, G. and H. Sun, Internalizing Congestion and Emissions Externality on Road Networks with Tradable Credits. *Procedia - Social and Behavioral Sciences*, Vol. 138, 2014, pp. 214–222.
36. Paipuri, M., E. Barmpounakis, N. Geroliminis, and L. Leclercq, Empirical observations of multi-modal network-level models: Insights from the pNEUMA experiment. *Transportation Research Part C: Emerging Technologies*, Vol. 131, 2021, p. 103300.
37. Ameli, M., J. P. Lebacque, and L. Leclercq, Evolution of multimodal final user equilibrium considering public transport network design history. *Transportmetrica B: Transport Dynamics*, Vol. 10, No. 1, 2022, pp. 923–953.
38. Idoudi, H., M. Ameli, C. N. Van Phu, M. Zargayouna, and A. Rachedi, An agent-based dynamic framework for population evacuation management. *IEEE Access*, Vol. 10, 2022, pp. 88606–88620.
39. Ameli, M., J.-P. Lebacque, and L. Leclercq, Simulation-based dynamic traffic assignment: Meta-heuristic solution methods with parallel computing. *Computer-Aided Civil and Infrastructure Engineering*, Vol. 35, No. 10, 2020, pp. 1047–1062.
40. Ameli, M., J.-P. Lebacque, and L. Leclercq, Cross-comparison of convergence algorithms to solve trip-based dynamic traffic assignment problems. *Computer-Aided Civil and Infrastructure Engineering*, Vol. 35, No. 3, 2020, pp. 219–240.
41. Ameli, M., *Heuristic Methods for Calculating Dynamic Traffic Assignment*. Ph.D. thesis, IFSTTAR Paris and Université de Lyon, 2019.
42. Alisoltani, N., M. Ameli, M. Zargayouna, and L. Leclercq, Space-time clustering-based method to optimize shareability in real-time ride-sharing. *Plos one*, Vol. 17, No. 1, 2022, p. e0262499.
43. Alisoltani, N., M. Zargayouna, and L. Leclercq, Data-oriented approach for the dial-a-ride problem. In *2019 IEEE/ACS 16th International Conference on Computer Systems and Applications (AICCSA)*, IEEE, 2019, pp. 1–6.
44. Amelia, M., N. Alisoltanib, and L. Leclercqb, Lyon Metropolis realistic trip data set including home to work trips with private vehicles during the morning peak. *URL: https://doi. org/10.25578/MLIDRM, doi*, Vol. 10, 2021.

45. Ameli, M., N. Alisoltani, and L. Leclercq, Lyon North realistic trip data set during the morning peak. *URL http://dx. doi. org/10.25578/HWN8KE*, 2021.
46. Chen, R., L. Leclercq, and M. Ameli, Unravelling System Optimums by trajectory data analysis and machine learning. *Transportation Research Part C: Emerging Technologies*, Vol. 130, 2021, p. 103318.
47. HERE Developer, 2020.
48. Ameli, M., J. P. Lebacque, and L. Leclercq, Day-to-day multimodal dynamic traffic assignment: Impacts of the learning process in case of non-unique solutions. In *DTA 2018, 7th International Symposium on Dynamic Traffic Assignment*, 2018, p. 5p.
49. Ameli, M., J. P. Lebacque, and L. Leclercq, Computational Methods for Calculating Multimodal Multiclass Traffic Network Equilibrium: Simulation Benchmark on a Large-Scale Test Case. *Journal of Advanced Transportation*, Vol. 2021, 2021.
50. Ameli, M., J.-P. Lebacque, and L. Leclercq, Multi-attribute, multi-class, trip-based, multimodal traffic network equilibrium model: Application to large-scale network. In *Traffic and Granular Flow'17 12*, Springer, 2019, pp. 487–495.
51. Ntziachristos, L., D. Gkatzoflias, C. Kouridis, and Z. Samaras, COPERT: A European road transport emission inventory model. *Environmental Science and Engineering (Subseries: Environmental Science)*, 2009, pp. 491–504.
52. Lejri, D., A. Can, N. Schiper, and L. Leclercq, Accounting for traffic speed dynamics when calculating COPERT and PHEM pollutant emissions at the urban scale. *Transportation Research Part D: Transport and Environment*, Vol. 63, 2018, pp. 588–603.